British Journal of Pharmacology (2005) 145, 503–513
www.nature.com/bjp

Prostaglandin E_2-induced modification of tetrodotoxin-resistant Na^+ currents involves activation of both EP_2 and EP_4 receptors in neonatal rat nodose ganglion neurones

*,[1]Shigeji Matsumoto, [1]Mizuho Ikeda, [1]Shinki Yoshida, [1]Takeshi Tanimoto, [1]Mamoru Takeda & [2]Masanori Nasu

[1]Department of Physiology, Nippon Dental University, School of Dentistry at Tokyo, 1-9-20 Fujimi, Chiyoda-ku, Tokyo 102-8159, Japan and [2]Research Center for Odontology, Nippon Dental University, School of Dentistry at Tokyo, Tokyo 102-8159, Japan

1 The aim of the present study was to investigate which EP receptor subtypes (EP_1–EP_4) act predominantly on the modification of the tetrodotoxin-resistant Na^+ current (I_{NaR}) in acutely isolated neonatal rat nodose ganglion (NG) neurones.

2 Of the four EP receptor agonists ranging from 0.01 to 10 μM, the EP_2 receptor agonist (ONO-AE1-259, 0.1–10 μM) and the EP_4 receptor agonist (ONO-AE1-329, 1 μM) significantly increased peak I_{NaR}. The responses were associated with a hyperpolarizing shift in the activation curve.

3 Neither the EP_1 receptor agonist ONO-DI-004 nor the EP_3 receptor agonist ONO-AE-248 significantly modified the properties of I_{NaR}.

4 In PGE_2 applications ranging from 0.01 to 10 μM, 1 μM PGE_2 produced a maximal increase in the peak I_{NaR} amplitude. The PGE_2 (1 μM)-induced increase in the $GV_{1/2}$ baseline (% change in G at baseline $V_{1/2}$) was significantly attenuated by either intracellular application of the PKA inhibitor PKI or extracellular application of the protein kinase C inhibitor staurosporine (1 μM). However, the slope factor k was not significantly altered by PGE_2 applications at 0.01–10 μM. In addition, the hyperpolarizing shift of $V_{1/2}$ by PGE_2 was not significantly altered by either PKI or staurosporine.

5 In other series of experiments, reverse transcription–polymerase chain reaction (RT–PCR) of mRNA from nodose ganglia indicated that all four EP receptors were present.

6 The NG contained many neuronal cell bodies (diameter <30 μm) with intense or moderate EP_2, EP_3, and EP_4 receptor-immunoreactivities.

7 These results suggest that the PGE_2-induced modification of I_{NaR} is mainly mediated by activation of both EP_2 and EP_4 receptors.

British Journal of Pharmacology (2005) **145,** 503–513. doi:10.1038/sj.bjp.0706212
Published online 11 April 2005

Keywords: Prostaglandin E_2; tetrodotoxin-resistant; EP receptor; nodose ganglion; RT–PCR; immunohistochemistry

Abbreviations: G–V, conductance–voltage; $GV_{1/2}$ baseline, percent change in conductance at baseline $V_{1/2}$; I–V, current–voltage; I_{NaR}, tetrodotoxin-resistant Na^+ current; k, slope factor; PGE_2, prostaglandin E_2; PKA, protein kinase A; PKC, protein kinase C; PKI, protein kinase inhibitor; TTX, tetrodotoxin; TTX-R, tetrodotoxin-resistant; NG, nodose ganglion; RT–PCR, reverse transcription–polymerase chain reaction

Introduction

It has been demonstrated that prostaglandin E_2 (PGE_2), one of the hyperalgesic agents, enhances the responsiveness of primary nociceptive neurones to bradykinin and/or capsaicin (Nicol & Cui, 1994; Cui & Nicol, 1995). Capsaicin-sensitive neurons in the dorsal root ganglion (DRG) preferentially express as the tetrodotoxin (TTX)-resistant voltage-gated Na^+ current (I_{NaR}), as compared with the case of capsaicin-insensitive neurones (Pearce & Duchen, 1994; Arbuckle & Docherty, 1995). In neurones expressing sensory neurone specific TTX-R channels, PGE_2 shifts the activation curve of the I_{NaR} to more negative potentials and enhances the amplitude of the current (England *et al*., 1996; Gold *et al*., 1998). These changes play an important role in determining the excitability of sensory TTX-R neurones. Electrophysiological properties of TTX-R Na^+ currents resemble those of the putative TTX-R 1 current referred to as the slow TTX-R current as well as the NaV 1.8 current (Rush *et al*., 1998; Scholz *et al*., 1998; Lai *et al*., 2002).

The nodose ganglion (NG) is known to contain primary sensory neurones, which receive afferent inputs from the cardiovascular, pulmonary, and gastrointestinal tracts. The majority of NG neurones have a slow conduction velocity (C type neurons) consistent with unmyelinated axons (Stansfeld & Wallis, 1985). During inflammatory reaction of the airways, autacoids, including prostaglandins, are locally released by a variety of cells, and PGE_2 is a particularly abundant prostanoid found in the lungs and airways during inflammation. The latter is confirmed by evidence demonstrating that during an asthmatic attack in human patients, PGE_2 levels in the

*Author for correspondence; E-mail: matsu-s@tky.ndu.ac.jp
Published online 11 April 2005

bronchoalveolar lavage increase by two- to 10-fold, compared with before the attack (Liu *et al*., 1988; Holtzman, 1991; Jörres *et al*., 1995). Furthermore, PGE_2 has a potentiating effect on the sensitivity of vagal C fiber activity in response to chemical or mechanical stimulation (Lee & Morton, 1995; Ho *et al*., 2000).

The multiformity of PGE_2 is thought to be responsible for the EP prostanoid receptor subtypes, EP_1–EP_4, coupled to different signal transduction pathways (Narumiya *et al*., 1999). In rat DRG nociceptive neurons, the sensitizing effect of PGE_2 is mediated by a protein kinase A (PKA) signal transduction, in which the activation of the EP_2, EP_3, or EP_4 receptor is involved (Lopshire & Nicol, 1998; Southall & Vasko, 2001). The EP_2, EP_3, and EP_4 receptors are linked to the activation of adenylate cyclase through Gs protein (Narumiya *et al*., 1999), and the sensitizing effects of PGE_2 occur as a result of the cAMP-PKA signal transduction mechanism, indicating that activation of the EP_2, EP_3, or EP_4 receptor may be involved (Cui & Nicol, 1995; Lopshire & Nicol, 1998; Smith *et al*., 2000). However, it is not well known how four subtypes of prostanoid receptor agonists, exhibiting the highest affinity for PGE_2 (Coleman *et al*., 1994; Narumiya *et al*., 1999), modify the excitability of NG neurones insensitive to TTX. The aim of the present study was to determine which EP receptor subtypes act predominantly on the PGE_2-induced modification of I_{NaR} in acutely isolated neonatal rat NG neurones. We therefore examined the effects of four selective EP receptor agonists and PGE_2 at different concentrations (0.01–10 μM) on I_{NaR}. In other series of experiments, expression of the four EP prostanoid receptors in the neonatal rat NG was examined by means of reverse transcription–polymerase chain reaction (RT–PCR). Finally, we examined which EP receptor subtypes are actually expressed in small-diameter NG neurones, by using the four EP receptor antibodies.

Methods

Cell culture

Primary cultures of dissociated neonatal NG neurones were prepared with the same technique as described in previous studies (Sahara *et al*., 1997; Ikeda & Matsumoto, 2003). In brief, Wistar rats (6–11 days, 14–26 g) were anaesthetized with pentobarbital sodium (50–60 mg kg^{-1}, i.p.). A pair of NG were dissected and incubated in modified Hank's balanced salt solution (HBSS) containing (in mM) 130 NaCl, 5 KCl, 0.3 KH_2PO_4, 4 $NaHCO_3$, 0.3 Na_2HPO_4, 5.6 glucose, and 10 HEPES. Then the dissected nodose ganglia were transferred to HBSS containing 20 U ml^{-1} of papain (Worthington Biochemical, NJ, U.S.A.) and incubated for 15–25 min at 37°C. Single cells were obtained by triturating the suspension through a wide-pore Pasteur pipette, and were subsequently plated onto poly-L-lysine pretreated glass coverslips in a 35-mm dish. The plating medium contained Leibovitz's L-15 solution (Invitrogen Corp, Carlsbad, CA, U.S.A.) supplemented with 10% newborn calf serum, 50 U ml^{-1} penicillin–streptomycin (Invitrogen Corp), 26 mM $NaHCO_3$, and 30 mM glucose. The cells were maintained in 5% CO_2 at 37°C and used for recording between 2 and 10 h after plating.

Recording solutions and drugs

The internal solution for electrodes consisted of (in mM): 10 NaCl, 100 CsF, 40 CsCl, 2 $MgCl_2$, 1 $CaCl_2$, 2 Mg-ATP, 10 HEPES, 14 Na_2 creatine-phosphate, and 11 EGTA; pH was adjusted to 7.2 with CsOH. The external solution consisted of (in mM): 30 NaCl, 80 choline-Cl, 40 tetraethylammonium (TEA)-Cl, 3 $MgCl_2$, 10 glucose, and 10 HEPES; pH was adjusted to 7.4 with TEAOH and the estimated concentration of Ca^{2+} in the pipette solution ranged 20–40 nM. In the voltage-clamp mode, solutions designed for the isolation of Na^+ currents were: (1) the external solution was Ca^{2+} free to prevent contamination of Na^+ currents from voltage-gated Ca^{2+} currents; (2) the external solution contained 30 mM NaCl to obtain the accuracy of Na^+ currents and to improve the fidelity of the voltage-clamp and the current obtained was completely abolished by replacement from 30 mM NaCl to 30 mM choline-Cl; (3) in the voltage-clamp mode, TTX (Sigma Chemical Co., St Louis, MO, U.S.A.) was added to the external solution and its concentration was adjusted to 1 μM. PGE_2 was obtained from Sigma Chemical Co. and dissolved in dimethylsulfoxide (DMSO). The DMSO concentration did not exceed 0.1%, and at this concentration it had no effect on the TTX-R Na^+ current. In some TTX-R NG neurones, no significant changes in the I_{NaR} were obtained in a Ca^{2+}-free solution perfusion without and with a Ca^{2+} channel blocker (Cd^{2+} concentration = 100 μM). ONO-DI-004 (EP_1 receptor agonist), ONO-AE1-259 (EP_2 receptor agonist), ONO-AE-248 (EP_3 receptor agonist) and ONO-AE1-329 (EP_4 receptor agonist) were kindly donated by Ono Pharmaceutical Co. Ltd (Osaka, Japan). Four EP receptor agonists were dissolved in DMSO (0.01%) and stored at −80°C.

Electrophysiological recording and pulse protocol

Electrophysiological recordings were performed with the whole-cell configuration of the patch-clamp technique (Hamill *et al*., 1981). For whole-cell voltage-clamp experiments, glass pipettes with a low resistance between 2 and 5 MΩ were used. Isolated cells on the glass coverslip were placed in a recording chamber and visualized by phase contrast on an inverted microscope (Nikon, Tokyo, Japan). The signal was measured with an Axopatch-1D patch-Clamp amplifier (Axon Instruments, Forster City, CA, U.S.A.). Data were low-pass-filtered at 5–10 kHz with a four-pole Bessel filter and digitally sampled at 25–100 kHz. After seal formation and membrane disruption, the whole-cell capacitance (10–20 pF) and series resistance (6–9 MΩ) were cancelled. The series resistance compensation (>80%) was employed. External solutions were applied *via* a linear array of seven polyethylene tubes (280 μm in diameter) mounted on a micromanipulator and positioned within 200 μm of cell bodies as described in previous studies (Sahara *et al*., 1997; Ikeda & Matsumoto, 2003). All NG neurons tested were less than 30 μm in diameter because I_{NaR} is preferentially expressed in small diameter NG neurones (Ikeda & Schofield, 1987; Schild & Kunze, 1997).

The current–voltage (*I–V*) relationship was first measured with step pulses (50 ms) from a holding potential (HP) of −80 mV to +40 mV in 5 mV increments at 5 s-intervals. Current was evoked from a −60 mV prepulse (10 ms) to an HP of −80 mV prior to each voltage clamp step. Under these conditions, the duration of the recordings were required to be 2 s. The changes in the conductance–voltage (*G–V*) relationship were constructed from the *I–V* curve by dividing the evoked current by the driving force on the current: $G = I\,(V_m - V_{rev})^{-1}$, where V_m is the potential at which the current was

evoked and V_{rev} is the reversal potential for the current. As reported by Saab *et al*. (2003), we found that the rapid increase in I_{NaR} amplitude occurred after rupture of the membrane. At 5 min after 1 μM TTX application, the amplitude of I_{NaR} was stabilized. After the application of TTX, we examined the changes in the peak I_{NaR} amplitude of the *I–V* curve at 5 min intervals for 15 min, by using some small diameter NG neurones.

Internal perfusion of PKA inhibitor

The internal perfusion of drugs was conducted by using the same technique as described in previous studies (Hori *et al*., 1999; Takahashi *et al*., 2000; Ishikawa *et al*., 2002). In brief, an Eppendorf yellow tip was heated and pulled to produce a tip diameter from 50 to 70 μm. The pipette solution containing an intracellular solution for measuring TTX-R Na^+ currents, a PKA inhibitor (protein kinase inhibitor, PKI, Sigma Chemical Co.) and a fluorescence dye Lucifer yellow (0.005%), was first back-filled into the tube, and then the intracellular solution was also back-filled into the tube for measuring their currents in the absence or the continuing presence of PGE_2. The tube was inserted into a patch pipette with its tip 500–600 μm behind the tip of the patch pipette. After obtaining control or PGE_2 responses, the dialysis solution was delivered into the patch pipette with positive pressure manually applied through a syringe. Under these conditions, there were no significant differences on the series resistance between before and during the internal perfusion of PKI. When Lucifer yellow was injected into a TTX-R NG neuron by this method, fluorescence became detectable within 2 min after injection and reached maximal intensity within an additional 4 min. The final concentration of the PKI in an Eppendorf yellow tip was determined by the magnitude of reduced baseline I_{NaR} ($>30\%$), by the effectiveness to completely inhibit the PGE_2-induced I_{NaR} increase, or by the magnitude of fluorescence in the presence of the preinjection volume of the pipette. Under these conditions, the magnitude of fluorescence was almost the same even though the concentration of PKI and the size of the cells recorded were verified. In the case of 1 mM PKI in an Eppendorf yellow tip, it greatly reduced the baseline I_{NaR} ($>50\%$), but at 10 μM of the PKA inhibitor, it had no significant effect on the two responses. The final concentration (100 μM) of PKI in an Eppendorf yellow tip had a moderate effect on baseline I_{NaR}, but effectively abolished PGE_2-induced modification of I_{NaR}. The injected volume of PKI ranged from 0.04 to 0.09 μl.

Data analysis and statistics

Data acquisition and analysis were carried out with the pCLAMP software (V6, Axon Instruments), Origin Soft (OriginLab Co., U.S.A.) and Microsoft Excel (Microsoft Co., U.S.A.). The normalized activation curve was fitted to GG_{max}^{-1} (the normalized conductance) $= 1\ \{1 + \exp\ [(V_{1/2} - V_m)\ k^{-1}]\}^{-1}$, by using the Boltzmann equation. V_m is the test pulse voltage, $V_{1/2}$ is the membrane potential at which 50% activation of the voltage is observed and k is the slope factor. Statistical analysis was performed with Student's *t*-test and/or one-way ANOVA with *Tukey's post hoc* test for paired samples.

To assess changes in the magnitude of conductance of I_{NaR} in response to PGE_2 application before and after the PKA or protein kinase C (PKC) inhibitor treatment, the effects of test agents were calculated by means of a percent change in G at baseline $V_{1/2}$ ($GV_{1/2}$ baseline). The value for G at $V_{1/2}$ before drug application was used as 100% for the calculation. Furthermore, statistical analysis of a difference between PKA and PKC inhibitors on the inhibition of PGE_2-induced $GV_{1/2}$ baseline modification was performed with Student's *t*-test for unpaired samples. Data were expressed as the means $\pm$ s.e.m. A value of less than 0.05 was considered statistically significant.

RNA isolation and RT–PCR

Total RNA was isolated from whole nodose ganglia of 11 neonatal rats (8 days, 18–20 g) with a Perfect RNA Eukaryotic kit (Eppendorf, Germany) (Wang *et al*., 2002). Total RNA was treated with DNAase I (Invitrogen, U.S.A.) at 37°C for 20 min to remove genomic DNA. The enzyme was blocked or removed by a phenol–chloroform extraction. Optical density readings were performed to estimate the amount of total RNA before the RT–PCR procedure.

The RT–PCR was conducted with the cMaster™ RT plus the PCR system kit (Eppendorf). A total of 4 μg of RNA and 2.5 ng random primer (Takara Shuzo Co. Ltd, Japan) were incubated at 65°C for 5 min and then cooled on ice. The primers used were for the EP_1 receptor (5′-CGCAGGGTTCA CGCACACGA-3′ and 5′-CACTGTGCCGGGAACTACGC-3′), for the EP_2 receptor (5′-AGGACTTCGATGGCAGAG GAGAC-3′ and 5′-CAGCCCCTTACACTTCTCCAATG-3′), for the EP_3 receptor (5′-CCGGGCACGTGGTGCTTCAT-3′ and 5′-TAGCAGCAGATAACCCAGG-3′), for the EP_4 receptor (5′-TTCCGCTCGTGGTGCGAGTGTTC-3′ and 5′-GAGGTGGTGTCTGCTTGGGTCAG-3′) and glyceraldehyde phosphatase dehydrogenase (GAPDH) (5′-CGGAGT CAACGGATTTGGTCGTAT-3′ and 5′-AGCCTTCTCCAT GGTGGTGAAGAC-3′). The RNA was reverse-transcribed at 42°C for 45 min, and RT was terminated by heating at 85°C for 5 min. PCR was performed in a 50 μl reaction volume containing 3 μl RT-product. Amplifications were performed in a standard Eppendorf Mastercycler with an initial denaturation step at 94°C for 2 min followed by 35 cycles. Each cycle consisted of a denaturation step at 94°C for 30 s, an annealing step at 63°C for 45 s, and an elongation step at 72°C for 60 s. This was followed by a final elongation step at 72°C for 10 min. The PCR products were then separated on a 1.5% agarose gel stained with syber green (Molecular Probe, U.S.A.).

Immunohistochemistry

In six rats, under artificial ventilation, the chest was widely opened at the middle. The animals were transcardially perfused with a fixative, consisting of 4% paraformaldehyde and 0.1 M phosphate-buffered saline (PBS, pH = 7.4), after perfusion with 0.9% NaCl solution (500 ml). The NG at both sides were removed. Following the fixation, serial sections with a thickness of 10 μm were cut in a cryostat (Kryostat 1720, Leica, Germany). Cryostat sections were mounted on APS-coated glass slides. Nonspecific immunoreactivity was inhibited by 5% skin milk in PBS for 20 min at room temperature.

Sections were exposed overnight to rabbit polyclonary antibodies for EP_1, EP_2, EP_3 and EP_4 receptors (1 : 1000, Caymanchem Com, U.S.A.), washed in 0.05% Tween 20 in PBS three times (5 min per time) and incubated for 24 h with secondary antibodies at room temperature. The fluorescently labeled secondary antibody used was Alexa® 568 goat anti-rabbit IgG (1 : 1000, Molecular Probes, U.S.A.). After the sections were rinsed in PBS, immunofluorescence was visualized by using the appropriate filters. Digital images were collected and stored on a laboratory computer and later analyzed with Adobe Photoshop ver. 7.0 and a Leica Imaging Analysis Tool. Conforcal images were generated in a Leica TCS NT laser scanning microscope (Leica).

Results

Time-dependent effect of internal fluoride on TTX-R Na^+ currents

To determine whether or not fluoride (F) contained in the internal solution induces the change in peak I_{NaR} as well as in the shift with time in the hyperpolarizing direction, we examined the time-dependent effects of F on I_{NaR}. After rupture of the membrane, the rapid increase in I_{NaR} occurred, and 5 min after 1 μM TTX application the amplitude of the current was stabilized. As shown in Figure 1a, no significant changes in TTX-R Na^+ currents evoked by depolarizing step pulses (−80 to +40 mV) were found at 5 min intervals for 15 min. Figure 1b–d showed the time course effect of internal F on I_{NaR} in six cells. The peak amplitude of I_{NaR} did not change significantly (Figure 1b, c). Values for the potential for 50% activation of the normalized G–V curve ($V_{1/2}$) and the slope factor (k) were −17.8±1.4 and 3.2±0.4 mV at 5 min after TTX (1 μM), −18.1±1.9 and 3.4±0.5 mV at 10 min after TTX, and −18.5±2.3 and 3.4±0.5 mV at 15 min after TTX (Figure 1d). Fluoride in the pipette solution had no significant effects on the background shift in the activation curve and the value for k. For 10 min recordings after the stabilization of I_{NaR}, the hyperpolarizing effect of activation curves was not observed.

Concentration-dependent effect of PGE_2 on TTX-R Na^+ currents

A typical example of the effects of PGE_2 at different concentrations (0.01–10 μM) on TTX-R Na^+ currents evoked by stepping pulses (−80 to +40 mV) is shown in Figure 2a. At 3 min after PGE_2 applications ranging from 0.01 to 1 μM, it caused enhancement of peak I_{NaR} amplitude of the I–V curve in a concentration-dependent manner. The PGE_2 application up to 10 μM did not cause any significant change on the peak I_{NaR} amplitude, as compared with that seen after 1 μM PGE_2 application. Figure 2b–d summarizes the effects of PGE_2 at different concentrations (0.01–10 μM) on I_{NaR} in six cells. The application of PGE_2 at 1 μM caused a maximal increase in the peak I_{NaR} (Figure 2b, c). Values for $V_{1/2}$ and k were −15.1±1.8 and 1.8±0.4 mV under control conditions, −16.7±2.0 and 2.0±0.5 mV after PGE_2 (0.01 μM), −17.7±1.8 ($P<0.05$) and 2.0±0.5 mV after PGE_2 (0.1 μM), −19.6±2.0 ($P<0.05$) and 2.0±0.6 after PGE_2 (1 μM), −20.7±2.0 ($P<0.05$) and 2.2±0.6 mV after PGE_2 (10 μM). The $V_{1/2}$ potential obtained after 1 μM PGE_2 application was 4.5 mV more negative than that before the application. PGE_2 at 10 μM shifted more negatively to 5.6 mV from control conditions (Figure 2d). Concerning the values for k after PGE_2 applications raging from 0.01 to 10 μM, there were no significant differences from the control values.

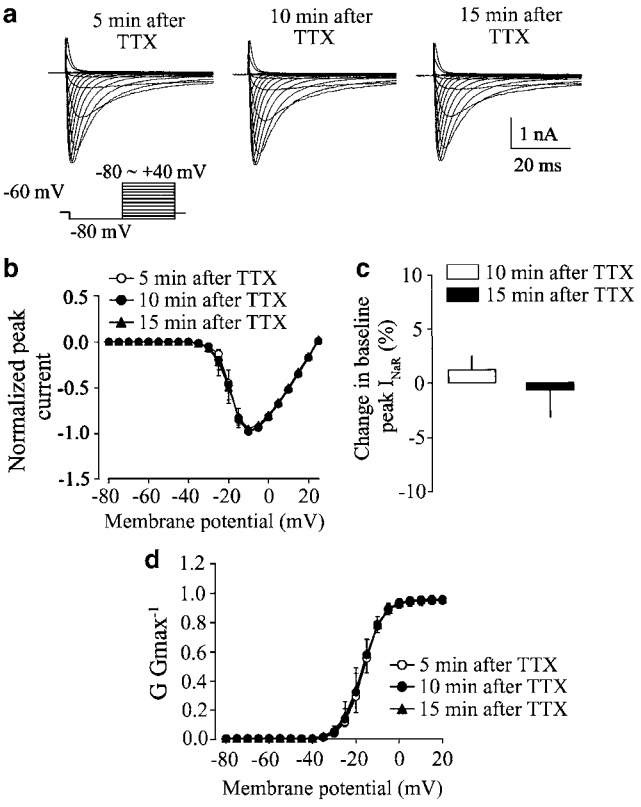

Figure 1 Internal F does not significantly alter basal TTX-R Na^+ currents. (a) TTX-R Na^+ currents were obtained at 5, 10 and 15 min after 1 μM TTX application. The cell was voltage-clamped at −80 mV and the currents were recorded by stepping the potential between −80 and +40 mV in 5 mV steps (duration of each step, 50 ms). Inset: voltage-pulse protocol. (b) Normalized current–voltage (I–V) curves were obtained at 5, 10 and 15 min. (c) Time-dependent effects of internal F on changes in peak I_{NaR} of the normalized I–V relationship, as compared with those after 5 min of 1 μM TTX application. (d) Normalized conductance–voltage (G–V) curves were obtained at 5, 10 and 15 min after 1 μM TTX application. Values are the means for six cells and the vertical bars show the s.e.m.

Effect of intracellular application of PKA inhibitor on the PGE_2-induced enhancement of TTX-R Na^+ currents

To examine whether PGE_2-induced enhancement of I_{NaR} is related to PKA-induced modification, we compared the effects of an intracellularly perfused PKI on the change in I_{NaR} as well as on the PGE_2-induced increase in $GV_{1/2}$ baseline (percent change in G at basal $V_{1/2}$). Before the intracellular PKI application, no fluorescence was observed. The PGE_2 (1 μM)-induced increase in I_{NaR} occurred at 3 min after the application. At 6 min after the internal application, fluorescence of the NG neurons became stable. The PKI in the continuing presence of 1 μM PGE_2 produced a significant decrease in I_{NaR} (Figure 3a). In seven cells, the intracellular application of PKI significantly attenuated the peak increase in the I_{NaR} amplitude induced by 1 μM PGE_2 application (Figure 3b, c). Values for

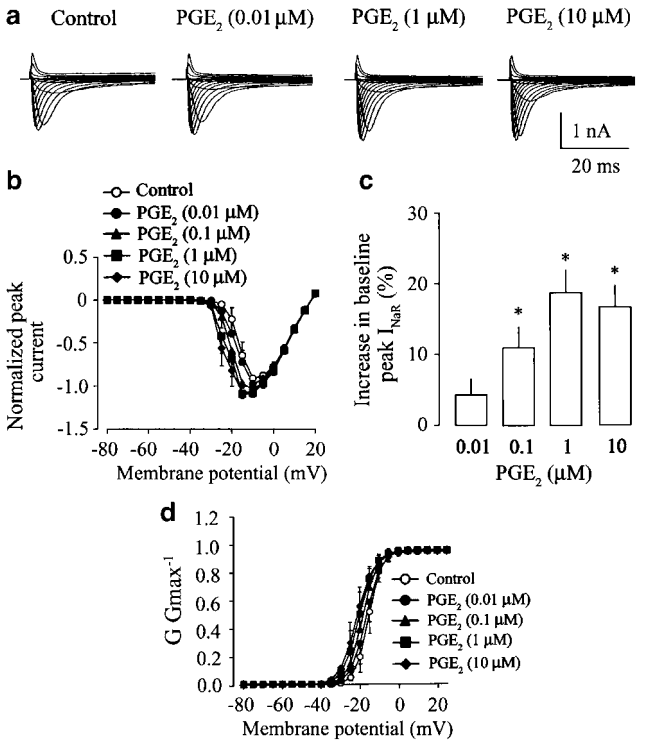

Figure 2 PGE_2 applications concentration-dependently enhance TTX-R Na^+ currents. (a) Typical I_{NaR} traces evoked by stepping pulses before and after application of PGE_2 at different concentrations (0.01, 1 and 10 μM). (b) Normalized current–voltage (I–V) curves were obtained after PGE_2 application at 0.01, 0.1, 1 and 10 μM. (c) Changes in peak I_{NaR} of the normalized I–V relationship before and after PGE_2 applications at 0.01, 0.1, 1 and 10 μM. (d) Normalized conductance–voltage (G–V) curves were obtained after PGE_2 application at 0.01, 0.1, 1 and 10 μM. Values are the means for six cells and vertical bars show the s.e.m. $^*P<0.05$, statistically significant difference from control values.

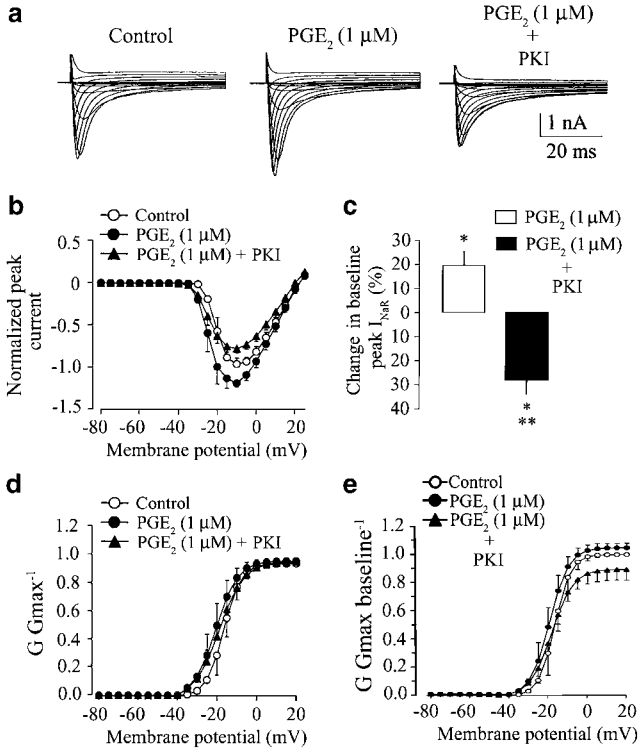

Figure 3 Intracellular application of PKI attenuated PGE_2-induced enhancement of I_{NaR}. (a) TTX-R Na^+ currents evoked from a representative cell under control conditions, after application of 1 μM PGE_2 and after internal application of protein kinase inhibitor (PKI) in the continuing presence of 1 μM PGE_2. (b) Normalized current–voltage (I–V) curves were obtained before and after 1 μM PGE_2 application in the absence and presence of a PKI internal perfusion. (c) Changes in peak I_{NaR} of the normalized I–V relationship after 1 μM PGE_2 application without and with a PKI internal perfusion. (d) Normalized conductance–voltage (G–V) curves were obtained before and after 1 μM PGE_2 application in the absence and presence a PKI internal perfusion. (e) G–V curves are plotted for data obtained before and after 1 μM PGE_2 application in the absence and presence of a PKI internal perfusion; data were normalized to the G_{max} baseline; Values are the means for seven cells and vertical bars show the s.e.m. $^*P<0.05$, statistically significant difference from control values. $^{**}P<0.05$, statistically significant difference from PGE_2 (1 μM) effects.

$V_{1/2}$ and k were -16.4 ± 2.1 and 1.9 ± 0.4 mV under control conditions, -20.4 ± 2.5 ($P<0.05$) and 2.1 ± 0.4 mV after PGE_2 (1 μM), -19.0 ± 2.2 ($P<0.05$) and 4.5 ± 0.7 mV ($P<0.05$) after application of both PGE_2 (1 μM) and PKI (Figure 3d). The hyperpolarizing shift of $V_{1/2}$ by PGE_2 (1 μM) was not significantly altered by internal PKI application but the values for k increased significantly. The PGE_2-induced increase in $GV_{1/2}$ baseline was $63.3\pm16.8\%$ in the absence of PKI but decreased by $-1.1\pm10.7\%$ ($P<0.05$, $n=7$) in its presence (Figure 3e). The intracellular application of PKI lowered the G_{max} to below the control level (prior to the PGE_2 application), indicating that there may be a difficulty to differentiate between a parallel effect of PKA inhibition and PGE_2 on I_{NaR}.

PKC-induced modification of TTX-R Na^+ currents

To determine whether PKC activity affects the properties of I_{NaR}, we examined the effects of PMA (one of the PKC activators) on I_{NaR} in the presence of staurosporine (one of the PKC inhibitors). Before staurosporine treatment, PMA application (0.1 μM) at a maximal concentration in the study to determine PKC-induced modification of I_{NaR} in adult TTX-R DRG neurons (Gold *et al*., 1998) caused an increase ($13.6\pm2.8\%$, $n=5$) in the peak current amplitude (data are not shown). In five cells, the values for $V_{1/2}$ and k were -15.4 ± 0.5 mV under control conditions and -18.8 ± 1.7 ($P<0.05$) and 3.7 ± 0.6 mV in the presence of 0.1 μM PMA. In the presence of staurosporine at 1 μM, PMA application (0.1 μM) had no effect on the TTX-R Na^+ currents evoked by stepping pulses (Figure 4a). In five cells, staurosporine blocked PMA-induced modification of I_{NaR} (Figure 4b, c). As shown in Figure 4c, staurosporine inhibited PMA-induced enhancement of I_{NaR}. Values for $V_{1/2}$ and k were -12.0 ± 1.2 and 3.8 ± 0.7 mV in the presence of staurosporine (1 μM) and -12.7 ± 1.3 and 3.8 ± 0.6 mV in the presence of both staurosporine (1 μM) and PMA (0.1 μM). No significant changes $V_{1/2}$ and k were found in the activation curve (Figure 4d).

Effect of a PKC inhibitor on the PGE_2-induced enhancement of TTX-R Na^+ currents

To determine whether PGE_2-induced enhancement of I_{NaR} is involved in the activation of PKC activity, we examined the effect of 1 μM PGE_2 on the change in I_{NaR} before and after additional application of staurosporine (1 μM). As shown in

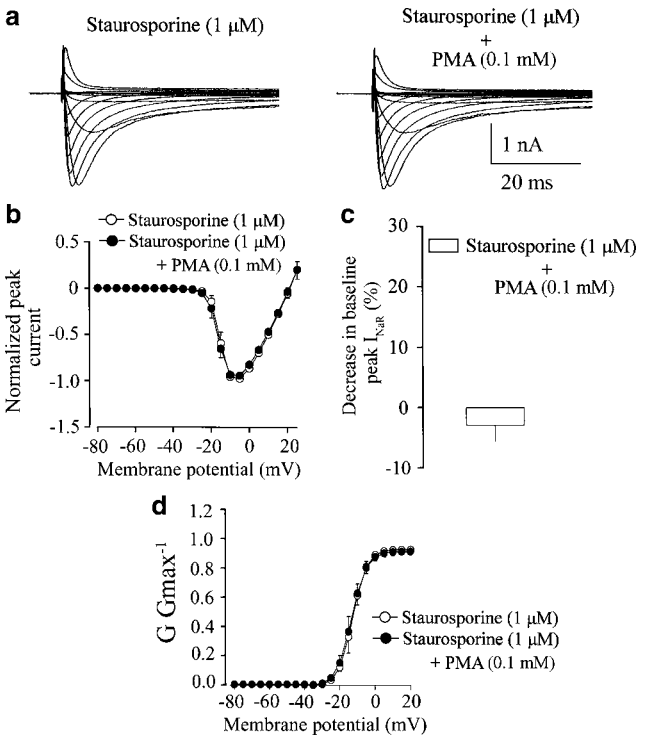

Figure 4 Staurosporine application antagonizes the effect of AMP on TTX-R currents. (a) Typical TTX-R Na^+ current traces evoked by 1 μM staurosporine before and after 0.1 μM PMA. (b) Normalized current–voltage (I–V) curves were obtained before and after 0.1 μM PMA in the continuing presence of 1 μM staurosporine. (c) Changes in peak I_{NaR} of the normalized I–V relationship in response to 0.1 μM PMA in the continuing presence of 1 μM staurosporine. (d) Normalized conductance–voltage (G–V) curves were obtained before and after 0.1 μM PMA in the continuing presence of 1 μM staurosporine. Values are the means for five cells and vertical bars show the s.e.m.

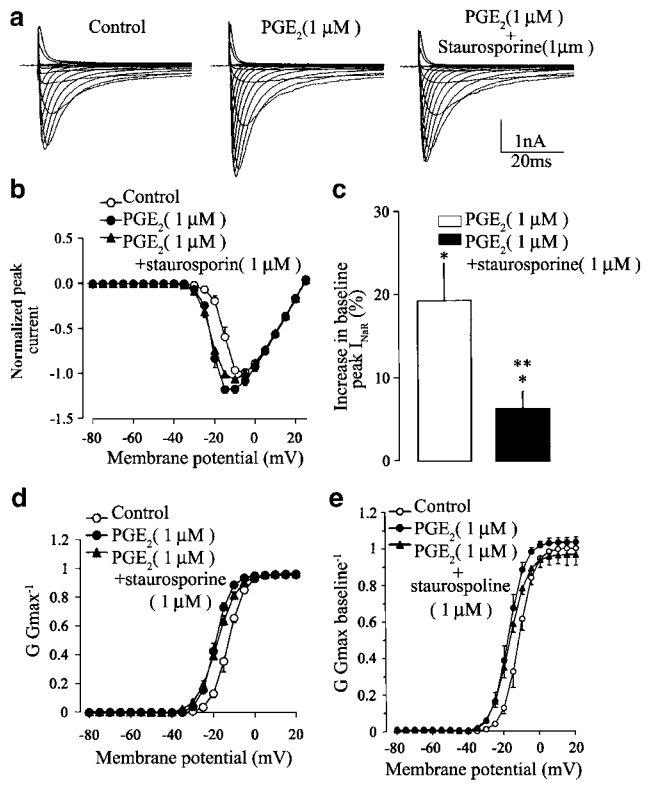

Figure 5 Additional staurosporine application alters PGE_2-induced modification of TTX-R currents. (a) Typical TTX-R Na^+ current traces evoked by 1 μM PGE_2 before and after 1 μM staurosporine application. (b) Normalized current–voltage (I–V) curves were obtained before and after 1 μM PGE_2 application in the absence and presence of 1 μM staurosporine. (c) Changes in peak I_{NaR} of the normalized I–V relationship and after 1 μM PGE_2 application without and with 1 μM staurosporine. (d) Normalized conductance–voltage (G–V) curves were obtained before and after 1 μM PGE_2 application in the absence and presence of 1 μM staurosporine. (e) G–V curves are plotted for data obtained before and after 1 μM PGE_2 application in the absence and presence of 1 μM staurosporine; data were normalized to the G_{max} baseline. Values are the means for six cells and vertical bars show the s.e.m. $^*P<0.05$, statistically significant difference from control values. $^{**}P<0.05$, statistically significant difference from PGE_2 (1 μM) effects.

Figure 5a, TTX-R Na^+ currents evoked by stepping pulses (-80–$+40$ mV) were enhanced by the application of 1 μM PGE_2, but this enhancement was significantly reduced by additional application of staurosporine (1 μM). Staurosporine attenuated PGE_2-induced increase in the peak I_{NaR} (Figure 5b, $n=6$). The values for $V_{1/2}$ and k were -13.1 ± 0.7 and 3.7 ± 0.5 mV under control conditions, -19.3 ± 0.8 ($P<0.05$) and 3.4 ± 0.4 mV after PGE_2 application (1 μM), -18.3 ± 0.9 ($P<0.05$) and 4.7 ± 0.2 mV ($P<0.05$) after application of both PGE_2 (1 μM) and staurosporine (1 μM) (Figure 5d). The PGE_2-induced hyperpolarizing shift in $V_{1/2}$ was not significantly affected by staurosporine application (1 μM), but under these conditions, the values for k increased significantly. The PGE_2-induced increase in $GV_{1/2}$ baseline was $62.1\pm6.7\%$ ($n=6$) in the absence of a PKC inhibitor but decreased by $37.1\pm6.3\%$ ($P<0.05$, $n=6$) in its presence. Staurosporine at 1 μM reversed the PGE_2 effect on the peak amplitude of I_{NaR} as well as the PGE_2-induced $GV_{1/2}$ baseline modulation, but had no significant effect on the hyperpolarization shift induced by PGE_2. The results indicate that the PKC pathway may not be involved in the PGE_2 response.

Effects of four EP receptors on TTX-R Na^+ currents

To determine which EP receptor subtypes contribute to PGE_2-induced enhancement of I_{NaR}, we examined the effects of selective agonists for EP_1, EP_2, EP_3 and EP_4 receptors on the current characteristics in neonatal NG neurones.

Typical examples of the effects of ONO-AE1-259, one of the EP_2 receptor agonists (0.01–10 μM), on TTX-Na^+ currents evoked by step pulses are shown in Figure 6a. At 3 min after ONO-AE1-259 applications at 0.1 and 1 μM, it caused enhancement of the peak I_{NaR}. The ONO-AE1-259 application up to 10 μM resulted in a slight reduction in peak I_{NaR}, compared with that seen after 1 μM application of the EP_2 receptor agonist. Figure 6b and c summarized the effect of ONO-AE1-259 (0.01–10 μM) on peak I_{NaR}. In 13 cells a maximal increase ($19.0\pm4.8\%$ $P<0.05$, $n=13$) in peak I_{NaR} was observed after 1 μM ONO-AE1-259 application and the response was associated with a hyperpolazing shift in the activation curve (Figure 6b–d). The value for $V_{1/2}$ potential was significantly hyperpolarized by 1 μM ONO-AE1-259 application (Figure 6d and Table 1).

The application of ONO-AE1-329, one of the EP_4 receptor agonists, at a concentration of 1 μM only increased TTX-R Na^+ currents evoked by step pulses (Figure 7a). In 13 cells,

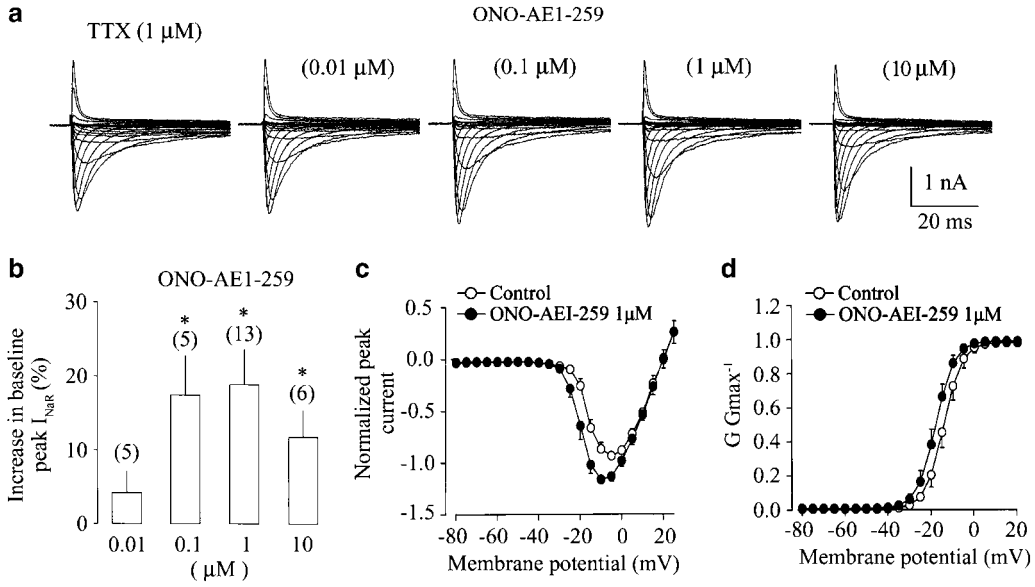

Figure 6 Effect of the EP_2 receptor agonist ONO-AE1-259 on TTX-R Na^+ currents. (a) Typical I_{NaR} traces evoked by stepping pulses before and after application of ONO-AE1-259 at different concentrations (0.01–10 μM). (b) Changes in peak I_{NaR} of normalized current–voltage (*I–V*) relationship before and after ONO-AE1-259 applications at 0.01, 0.1, 1 and 10 μM; (*n*) = the number of cells. (c) Normalized *I–V* curves were obtained before and after 1 μM ONO-AE1-259 application. (d) Normalized conductance–voltage (*G–V*) curves were obtained before and after 1 μM ONO-AE1-259 application. Values are the means for 13 cells and vertical vars show the s.e.m. $*P<0.05$, statistically significant difference from control values.

1 μM ONO-AE1-329 application significantly increased peak I_{NaR} (Figure 7b, c). As summarized in Figure 7d and Table 1, ONO-AE1-329 at 1 μM produced a significant increase in peak I_{NaR} and resulted in a significant hyperpolarization of the $V_{1/2}$ value for activation.

As shown in Table 1, the values for $V_{1/2}$ and k were not significantly altered by either the EP_1 receptor agonist ONO-DI-004 (1 μM) or the EP_3 receptor agonist ONO-AE-248 (1 μM) application.

Furthermore, application of both the EP_1 receptor agonist ONO-DI-004 (0.01–10 μM) and the EP_3 receptor agonist ONO-AE-248 (0.01–10 μM) had little or no effect on TTX-R Na^+ currents evoked by step pulses (data are not shown).

The expression of prostanoid receptor mRNA in the NG

The expression of the four prostanoid EP receptors (EP_1, EP_2, EP_3 and EP_4 receptors) in the neonatal NG was examined with the RT–PCR technique. Messenger RNA was isolated from the NG of 11 neonatal rats, and PCR was performed with the primers shown in Methods. The primers selectively amplified mRNA fragments of the expected size (Figure 8a–f). The mRNA for EP_1 (b), EP_2 (c), EP_3 (d) and EP_4 (e) receptors was found, but EP_1 receptor mRNA was weakly amplified.

Prostanoid receptor-immunoreactive neurones in the NG

As shown in Figure 9, the NG contained few EP_1 receptor-immunoreactive neurons; 11.3% of NG neurones were immunoreactive for EP_1 (a) receptors. The NG contained many neuronal cell bodies with intense or moderate EP_2 (b), EP_3 (c) and EP_4 (d) receptor-immunoreactivities; 70.9, 82.0 and 64.8% of NG neurons were immunoreactive for EP_2, EP_3 and EP_4 receptors, respectively (Figure 9a–d). The positive immunoreactivities to the EP_1–EP_4 receptor proteins were mostly found in the small size neurone, below 30 μm in diameter.

Table 1 Effects of four EP receptor agonists on the kinetics of I_{NaR}

Test agent	n	$V_{1/2}$ *for activation* (mV)	*Slope factor* (mV)
Control	11	−14.4±1.4	2.3±0.4
ONO-DI-004 (1 μM)	11	−16.7±1.8	2.2±0.5
Control	13	−13.3±1.4	2.9±0.5
ONO-AE1-259 (1 μM)	13	−17.9±1.5[a]	3.0±0.4
Control	10	−15.0±1.4	1.7±0.2
ONO-AE-248 (1 μM)	10	−16.3±1.5	2.0±0.3
Control	13	−14.5±1.0	3.0±0.4
ONO-AE1-329 (1 μM)	13	−18.0±1.2[a]	3.0±0.4

Data are expressed as the means±s.e.m.
[a]Significant differences between control and experimental groups ($P<0.05$).

Discussion

About 10% of NG neurons have myelinated axons and they typically exhibit rapidly rising action potentials that are completely abolished by TTX application (Stansfeld & Wallis, 1985; Seagard *et al*., 1990; Undem & Weinreich, 1993). Although most NG neurons express both TTX-S and TTX-R currents, we used a fraction of neurons with predominant TTX-R Na^+ currents in the continuing presence of 1 μM TTX, as suggested by Fazan *et al*. (2001).

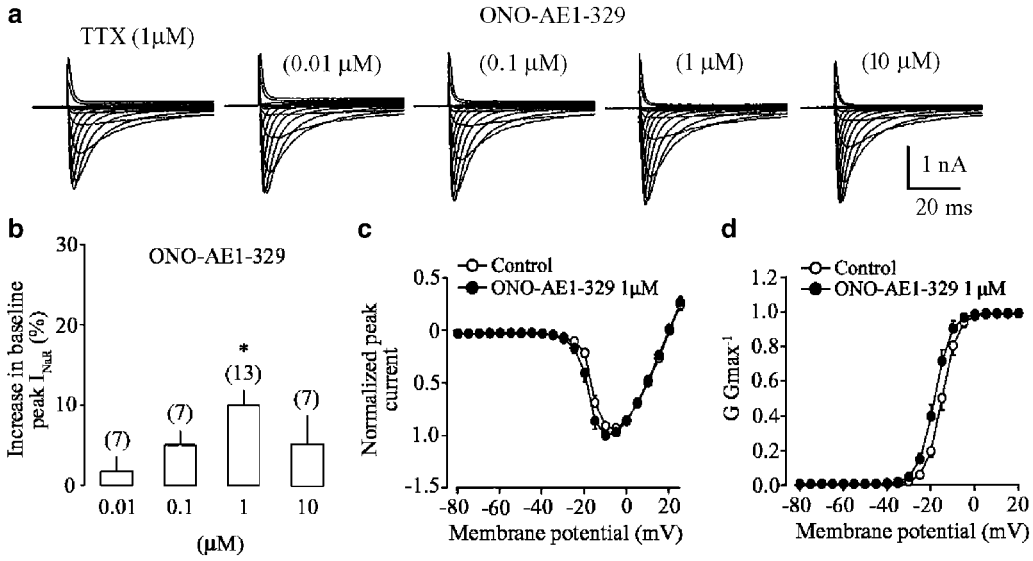

Figure 7 Effect of the EP_4 receptor agonist ONO-AE1-329 on TTX-R Na^+ currents. (a) Typical I_{NaR} traces evoked by stepping pulses before and after application of ONO-AE1-329 at different concentrations (0.01–10 μM). (b) Charges in peak I_{NaR} of the normalized current–voltage (*I–V*) relationship before and after ONO-AE1-329 applications at 0.01, 0.1, 1 and 10 μM; (*n*) = the number of cells. (c) Normalized *I–V* curves were obtained before and after 1 μM ONO-AE1-239 application. (d) Normalized conductance–voltage (*G–V*) curves were obtained before and after 1 μM ONO-AE1-239. Values are the means for 13 cells and the vertical bars show the s.e.m. $*P<0.05$, statistically significant difference from control values.

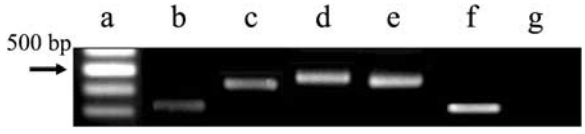

Figure 8 Example of mRNA cording of four EP receptors in neonatal nodose ganglia. Gel electrophoresis of PCR products obtained from nodose ganglia. Lane a, a nucleotide size ladder in 100 bp increments. Lanes b, c, d and e, PCR products obtained with the primers for EP_1 (336 bp), EP_2 (401 bp), EP_3 (437 bp) and EP_4 (423 bp) receptor, respectively. Lane f, PCR products obtained with the primers for GAPDH (306 bp). Lane g, negative control (no reverse transcription).

England *et al.* (1996) reported that the modification of TTX-R Na^+ currents after the application of PGE_2 or dibutyryl cAMP (db-cAMP) persisted after the removal of the drugs and this modifying effect was very slow to reverse the baseline I_{NaR}. In the present study, we obtained similar effects of PGE_2 on I_{NaR}. The recovery process of PGE_2 on I_{NaR} was very slow and this process may affect I_{NaR} cteristics such as hyperpolarization shift even in the absence and presence of a membrane permeant PKA inhibitor. To avoid such an effect and to determine whether PKA activation is actually involved in PGE_2-induced modification of I_{NaR}, we examined the inhibitory effects of internal PKI at a relatively smaller concentration or volume on I_{NaR} in the continuing presence of PGE_2. A PKA inhibitor, PKI, applied intracellularly greatly attenuated the PGE_2-induced increase in I_{NaR} as well as the mean percent increase in $GV_{1/2}$ baseline induced by PGE_2, but had no significant effect on the values for the $V_{1/2}$ potential of the activation curve compared with those before PKI application. The fact that the hyperpolarizing shift in the activation curve was still present in combination of PGE_2 with a PKA inhibitor led us to suggest that the PGE_2-induced modification of the I_{NaR} characteristics may not involve the activation of PKA. In addition, we found that staurosporine, one of the PKC inhibitors, at a concentration of 1 μM could inhibit PGE_2-mediated increase in the peak I_{NaR}. Although staurosporine at 1 μM is known to block a broad spectrum kinase, for example, PKC, PKA, Ca^{2+}-calmodulin kinase, protein kinase G and myosin light chain kinase (Ruegg & Burgess, 1989), we found that staurosporine (1 μM) could antagonize the effects of a potent PKC activator PMA (0.1 μM). The PGE_2-induced increase in the $GV_{1/2}$ baseline was significantly reduced by extracellular application of staurosporine (1 μM), but the response was associated with the hyperpolarization shift of $V_{1/2}$. The results suggest that there may be other pathways independent of PKC activity. Based on evidence that a significant inhibition of PGE_2-induced increases in the peak current amplitude and $GV_{1/2}$ baseline was seen in the continuing presence of a PKA or PKC inhibitor, it cannot completely rule out the possibility that the PGE_2-induced enhancement of I_{NaR} characteristics is at least in part involved in the activation of PKA or PKC.

PGE_2 binds to specific prostanoid receptors on target cells and is then rapidly removed by prostaglandin transporters on various cells (Schuster, 1998). Also, PGE_2 receptors are basically divided into four subtypes to exhibit the highest affinity: EP_1, EP_2, EP_3 and EP_4 (Coleman *et al.*, 1994; Narumiya *et al.*, 1999). Determination of the EP receptor subtype involving the PGE_2-induced modification of I_{NaR} is not easy because there are no selective EP antagonists at present. However, four EP receptor agonists, ONO-DI-004 (EP_1 receptor), ONO-AE1-259 (EP_2 receptor), ONO-AE-249 (EP_3 receptor) and ONO-AE1-329 (EP_4 receptor), have been recently developed, and they have little effect even at concentrations 1000 times higher than their respective K_i values when tested on Chinese hamster ovary (CHO) cells expressing other EP receptors (Suzawa *et al.*, 2000). The results indicate that the four EP receptor agonists are potent and selective. Then, of the four EP receptor agonists tested,

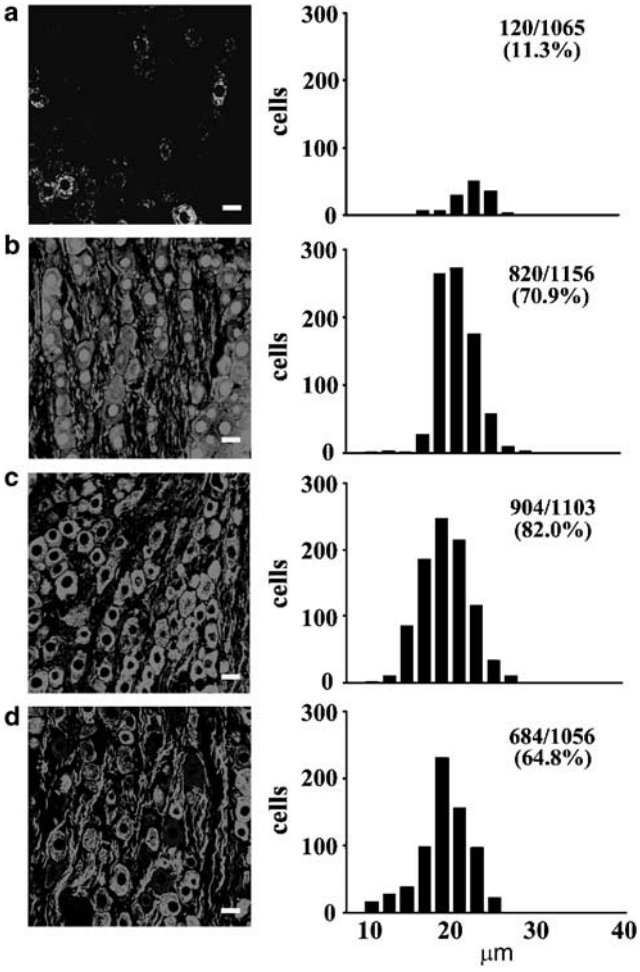

Figure 9 Immunofluorescence staining of neonatal rat nodose ganglion neurones and histograms showing diameters of cells labeled with four EP (EP_1, EP_2, EP_3 and EP_4) receptor-specific antibodies. Scale bars are 20 μm.

ranging from 0.01 to 10 μM, we found that the EP_2 receptor agonist ONO-AE1-259 (0.1, 1 and 10 μM) and the EP_4 receptor agonist ONO-AE1-329 (1 μM) could mimick the PGE_2-induced modification of I_{NaR}, which was characterized by an increase in the peak I_{NaR} and by a hyperpolarizing shift in the activation curve. These results show that stimulation of EP_2 and/or EP_4 receptors may increase cAMP, which is an effective stimulus for the I_{NaR}. Based on evidence that the mouse cDNA previously reported as a PGE_2 receptor EP_2 subtype (Honda *et al*., 1993) was identical to the pharmacologically defined EP_4 subtype (Nishigaki *et al*., 1995), our data reported here indicate that the effect of PGE_2 on the TTX-R I_{Na} in the neonatal NG neuron involves activation of both EP_2 and EP_4 receptors. In comparison with the potency of EP_2 and EP_4 receptor agonists on I_{NaR}, we found that a significant increase in the peak I_{NaR} amplitude occurred at lower concentrations of an EP_2 receptor agonist. This finding is consistent with the observation that the effect of PGE_2 may appear mainly through activation of EP_2 receptors in pulmonary C neurons, corresponding to TTX-R neurons in the nodose and jugular ganglia (Kwong & Lee, 2002). In fact, they reported that in pulmonary C neurons identified by retrograde labeling with a fluorescent tracer, butaprost (3–10 μM), a selective EP_2 receptor agonist, augmented the whole-cell current density elicited by capsaicin and increased the number of action potentials evoked by a depolarizing step pulse in a similar manner to that seen after PGE_2 application (1 μM). As butaprost cannot bind EP_1, EP_3 or EP_4 receptors at 3–10 μM (Boie *et al*., 1997; Kiriyama *et al*., 1997), it is possible that the effect of PGE_2 on the neonatal NG neurons insensitive to TTX may be mainly mediated by activation of EP_2-like receptors. This was further supported by the fact that the effect of ONO-AE1-259 (a EP_2 receptor agonist) on I_{NaR} was much more pronounced than that of ONO-AE1-329 (a EP_4 receptor agonist).

In other series of experiments, the mRNA for all four EP receptors was found in all animals examined, but the PCR reaction of the EP_1 receptor mRNA was less efficient. The agonist selective for EP_1 receptor, ONO-DI-004, ranging from 0.01 to 10 μM had no significant effect on the peak I_{NaR}. We also found that there were only 11.3% of EP_1 receptor immunoreactive neurons in the whole NG. These results lead us to suggest that the activation of EP_1 receptors would not importantly contribute to PGE_2-induced modification of I_{NaR} in the majority of cells in the NG. We could not completely rule out the possibility that EP_1 receptors may play a significant role in modulation of I_{NaR} in the 11.3% of cells that expressed I_{NaR}. The higher density of EP_3 receptor mRNA and the higher percentage (>80%) of EP_3 receptor immunoreactive neurons in the whole NG were found, but application of a selective EP_3 receptor agonist, ONO-AE-248 (0.01–10 μM), had little or no effect on the peak I_{NaR}. The results indicate that the EP_3 receptor subtype may not function in PGE_2-mediated I_{NaR} modification. However, there is a report that the inhibitory effect of PGE_2 on the high voltage-activated (HVA) Ca^{2+} current in acutely isolated trigeminal neurons is mimicked by the EP_3 receptor agonist, but not by the EP_1, EP_2 and EP_4 receptor agonists, irrespective of T-type Ca^{2+} currents (Borgland *et al*., 2002). It has been reported that Ca^{2+}-activated K^+ currents have the potential to modify the firing pattern and neuronal firing rate (Cordoba-Rodriguez *et al*., 1999). Thus, it can be suggested that application of the EP_3 receptor agonist ONO-AE-248 decreases the Ca^{2+}-activated K^+ current through the inhibition of HVA channels, resulting in an increase in the spike frequency. Further studies are needed to elucidate whether or not the EP_3 receptor agonist modifies the Ca^{2+}-activated K^+ current and this current contributes to the changes in action potentials of TTX-R NG neurons induced by ONO-AE-248, one of the EP_3 receptor agonists.

Although it has been recently demonstrated that fluoride (F) in the internal solution has several actions without components, such as PKA and PKC, of intracellular second messengers in small diameter DRG neurones (Saab *et al*., 2003), we could not find any significant difference comparing F effects on the amplitude of I_{NaR} and the shift in the activation curve at 5 min to recordings obtained with those at 10 or 15 min. This supports the idea that time-dependent (10 min) effects of F in the pipette solution may not have either specific effects on I_{NaR} or the background shift of the activation for I_{NaR}. In NG neurones insensitive to TTX, slow inactivation of the I_{NaR} occurs after trains of brief depolarizations and the recovery from its effect requires minutes to reach a steady state (Fazan *et al*., 2001). In this study, we obtained evidence that although a −60 mV step pulse, lasting for 10 ms, preceded by −80 mV HP was applied between −80 and

+40 mV in 5 mV increments, neither *I–V* nor activation curve relationships were significantly changed at 5 min intervals for 15 min. The results of the voltage clamp data suggest that slow inactivation has little or no effect on I_{NaR} in this study.

In conclusion, our results demonstrate that the increase in I_{NaR} induced by PGE_2 application may not involve the activation of either PKA or PKC activity, but is mediated by the activation of both EP_2 and EP_4 receptors.

References

ARBUCKLE, J.B. & DOCHERTY, R.J. (1995). Expression of tetrodotoxin-resistant sodium channels in capsaicin-sensitive dorsal root ganglion neurons of adult rats. *Neurosci. Lett.,* **185,** 70–73.

BOIE, Y., STOCCO, R., SAWYER, N., SLIPETZ, D.M., UNGRIN, M.D., NEUSCHÄFER-RUBE, F., PÜSCHEL, G.P., METTERS, K.M. & ABRAMOVITZ, M. (1997). Molecular cloning and characterization of the four rat prostaglandin E2 prostanoid receptor subtypes. *Eur. J. Pharmacol.,* **340,** 227–241.

BORGLAND, S.L., CONNOR, M., RYAN, R.M., BALL, H.J. & CHRISTIE, M.J. (2002). Prostaglandin E_2 inhibits calcium current in two sub-population of acutely isolated mouse trigeminal sensory neurons. *J. Physiol. (London),* **539,** 433–444.

COLEMAN, R.A., SMITH, W.L. & NARUMIYA, S. (1994). International Union of Pharmacology classification of prostanoid receptors: properties, distribution, and structure of the receptors and their subtypes. *Pharmacol. Rev.,* **46,** 205–229.

CORDOBA-RODRIGUEZ, R., MOORE, K.A., KAO, J.P. & WEINREICH, D. (1999). Calcium regulation of a slow post-spike hyperpolarization in vagal afferent neurons. *Proc. Natl. Acad. Sci. U.S.A.,* **96,** 7650–7657.

CUI, M. & NICOL, G.D. (1995). Cyclic AMP mediates the prostaglandin E_2-induced potentiation of bradykinin excitation in rat sensory neurons. *Neuroscience,* **66,** 459–466.

ENGLAND, S., BEVAN, S. & DOCHERTY, R.J. (1996). PGE_2 modulates tetrodotoxin-resistant sodium current in neonatal rat dorsal root ganglion neurons *via* the cyclic AMP-protein kinase A cascade. *J. Physiol. (London),* **459,** 429–440.

FAZAN JR, R., WHITEIS, C.A., CHAPLEAU, M.W., ABBOUD, F.M. & BIELEFELDT, K. (2001). Slow inaction of sodium currents in the rat nodose neurons. *Auton. Neurosci-Basic,* **87,** 209–216.

GOLD, M.S., LEVINE, D.J. & CORREA, A.M. (1998). Modulation of TTX-R INa by PKC and PKA and their role in PGE_2-induced sensitization of rat sensory neurons *in vitro*. *J. Neurosci.,* **18,** 10345–10355.

HAMILL, O.P., MARTY, A., NEHER, E., SAKMANN, B. & SIGWORTH, F.J. (1981). Improved patch-clamp techniques for high-resolution current recording from cells and cell-free membrane patches. *Pflügers. Archiv.,* **391,** 1108–1112.

HO, C.Y., GU, Q., HONG, J.L. & LEE, L.-Y. (2000). Prostaglandin E_2 enhances chemical and mechanical sensitivities of pulmonary C fibres in the rat. *Am. J. Respir. Crit. Care. Med.,* **162,** 528–533.

HOLTZMAN, M.J. (1991). Arachidonic acid metabolism. Implications of biological dhemistry for lung function and disease. *Am. Rev. Respir. Dis.,* **143,** 188–203.

HONDA, A., SUGIMOTO, Y., NAMBA, T., WATANABE, A., IRIE, A., NEGISHI, M., NARUMIYA, S. & ICHIKAWA, A. (1993). Cloning and expression of a cDNA for mouse prostaglandin EP_2 subtype. *J. Biol. Chem.,* **268,** 7759–7762.

HORI, T., TAKAI, Y. & TAKAHASHI, T. (1999). Presynatic mechanism for phorbol estel-induced synaptic potentiation. *J. Neurosci.,* **19,** 7262–7267.

ISHIKAWA, T., SAHARA, Y. & TAKAHASHI, T. (2002). A single packet of transmitter does not saturate postsynaptic glutamate receptors. *Neuron,* **34,** 613–621.

IKEDA, M. & MATSUMOTO, S. (2003). Classification of voltage-dependent Ca^{2+} channels in trigeminal ganglion neurons from neonatal rats. *Life Sci.,* **73,** 1175–1187.

IKEDA, S.R. & SCHOFIELD, G.G. (1987). Tetrodotoxin-resistant sodium current of rat nodose neurons: monovalent cation selectivity and divalent cation block. *J. Physiol. (London),* **389,** 255–270.

JÖRRES, R., NOWAK, D., GRIMMINGER, F., SEEGER, W., OLDIGS, M. & MAGNUSSEN, H. (1995). The effect of 1 ppm nitiogen dioxide on broncho alveolar lavage cells and inflammatory mediators in normal and asthmatic subjects. *Eur. Respir. J.,* **8,** 416–424.

KIRIYAMA, M., USHIKUBI, F., KOBAYASHI, T., HIRATA, M., SUGIMOTO, Y. & NARUMIYA, S. (1997). Ligand binding specificities of the eight types and subtypes of the mouse prostanoid receptors expressed in Chinese hamster ovary cells. *Br. J. Pharmacol.,* **122,** 217–224.

KWONG, K. & LEE, L.-Y. (2002). PGE_2 sensitizes cultured pulmonary vagal sensory neurons to chemical and electrical stimuli. *J. Appl. Physiol.,* **93,** 1419–1428.

LAI, J., GOLD, M.S., KIM, C.-S., BIAN, D., OSSIPOV, M.H., HUNTER, J.C. & PORRECA, F. (2002). Inhibition of neuropathic pain by decreased expression of the tetrodotoxin-resistant sodium channel, NaV 1.8. *Pain,* **79,** 143–152.

LEE, L.-Y. & MORTON, R.F. (1995). Pulmonary chemoreflex sensitivity is enhanced by prostaglandin E_2 in anesthetized rats. *J. Appl. Physiol.,* **79,** 1679–1686.

LIU, M.C., BLEECKER, E.R., PROUD, D., MCLEMORE, T.L. & HUBBARD, W.C. (1988). Profiling of bisenoic prostaglandins and thromboxane B_2 in bronchoalveolar fluid from the lower respiratory tract of human subjects by combined capillary gas chromatographymass-mass spectrometry. *Prostaglandins,* **35,** 67–79.

LOPSHIRE, J.C. & NICOL, G.D. (1998). The cAMP transduction cascade mediates the prostaglandin E_2 enhancement of the capsaicin-elicited current in rat sensory neurons: whole-cell and single-channel studies. *J. Neurosci.,* **18,** 6081–6092.

NARUMIYA, S., SUGIMOTO, Y. & USHIKUBI, F. (1999). Prostanoid receptors: structures, properties, and functions. *Physiol. Rev.,* **79,** 1193–1226.

NICOL, G.D. & CUI, M. (1994). Enhancement by prostaglandin E_2 of bradykinin activation of embryonic rat sensory neurons. *J. Physiol. (London),* **480,** 485–492.

NISHIGAKI, N., NEGISHI, M., HONDA, A., SUGIMOTO, Y., NANBA, T., NARUMIYA, S. & ICHIKAWA, A. (1995). Identification of prostaglandin E receptor 'EP_2' cloned from mastocytoma cells as EP_4 subtype. *FEBS Lett.,* **364,** 339–341.

PEARCE, R.J. & DUCHEN, M.R. (1994). Differential expression of membrane currents in dissociated mouse primary sensory neurons. *Neuroscience,* **63,** 1041–1056.

RUEGG, U.T. & BURGESS, G.M. (1989). Staurosporine, K-252 and UCN-01: potent but nonspecific inhibitors of protein kinases. *Trends. Pharmacol. Sci.,* **10,** 218–220.

RUSH, A.M., BRÄU, M.E., ELLIOTT, A.A. & ELLIOTT, J.R. (1998). Electrophysiological properties of sodium current subtypes in small cells from adult rat dorsal root ganglia. *J. Physiol. (London),* **511,** 771–789.

SAAB, C.Y., CUMMINS, T.R. & WAXMAN, S.G. (2003). GTPγs increases Nav 1.8 current in small-diameter dorsal root ganglia neurons. *Exp. Brain. Res.,* **152,** 415–419.

SAHARA, Y., NORO, N., IIDA, Y., SOMA, K. & NAKAMURA, Y. (1997). Glutamate receptor subunits GluR5 and KA-2 are coexpressed in rat trigeminal ganglion neurons. *J. Neurosci.,* **17,** 6611–6620.

SCHILD, J.H. & KUNZE, D.L. (1997). Experimental and modeling study of Na^+ current heterogeneity in rat nodose neurons and its impact on neuronal discharge. *J. Neurophysiol.,* **78,** 3198–3209.

SCHOLZ, A., APPE, N. & VOGEL, W. (1998). Two types of TTX-resistant and one TTX-sensitive Na^+ channel in rat dorsal root ganglion neurons and their blockade by halothane. *Eur. J. Neurosci.,* **10,** 2547–2556.

SCHUSTER, V.L. (1998). Molecular mechanisms of prostaglandin transport. *Annu. Rev. Physiol.,* **60,** 221–242.

SEAGARD, J.L., VAN BREDERODE, J.F.M., DEAN, C., HOPP, F.A., GALLENBERG, L.A. & KAMPINE, J.P. (1990). Firing characteristics of single-fiber carotid sinus baroreceptors. *Circ. Res.,* **66,** 1499–1509.

SMITH, J.A., DAVIS, C.L. & BURZESS, G.M. (2000). Prostaglandin E_2-induced sensitization of bradykinin-evoked responses in rat dorsal root ganglion neurons is mediated by cAMP-dependent protein kinase A. *Eur. J. Neurosci.,* **12,** 3250–3258.

SOUTHALL, M.D. & VASKO, M.R. (2001). Prostaglandin receptor subtypes, EP_{3C} and EP_4, mediate the prostaglandin E_2-induced cAMP production and sensitization of sensory neurons. *J. Biol. Chem.,* **276,** 16083–16091.

STANSFELD, C.E. & WALLIS, D.I. (1985). Properties of visceral primary afferent neurons in the nodose ganglion of the rabbit. *J. Neurophysiol.,* **54,** 245–260.

SUZAWA, T., MIYAURA, C., INADA, M., MARUYAMA, T., SUGIMOTO, Y., USHIKUBI, F., ICHIKAWA, A., NARUMIYA, S. & SUDA, T. (2000). The role of prostaglandin E receptor subtypes (EP_1, EP_2, EP_3, and EP_4) in bone resorption: an analysis using specific agonists for the respective EPs. *Endocrinology,* **141,** 1554–1559.

TAKAHASHI, T., HORI, T., KAJIKAWA, Y. & TSUJIMOTO, T. (2000). The role of GTP-binding protein activity in fast central synaptic transmission. *Science,* **289,** 460–463.

UNDEM, B.J. & WEINREICH, D. (1993). Electrophysiological properties and chemosensitivity of guinea pig nodose neurons *in vitro*. *J. Auton. Nerv. Syst.,* **44,** 17–34.

WANG, E.Q., LEE, W.-I., BRAZEAU, D. & FUNG, H.-L. (2002). cDNA microarray analysis of vascular gene expression after nitric oxide donor infusions in rats: implications for nitrate tolerance mechanisms. *AAPS. Pharm. Sci.,* **4,** E10.

(Received November 19, 2004
Revised February 1, 2005
Accepted February 24, 2005)